652 *Inorg. Chem.* **1999,** *38,* 652−660

Solid State and Solution Structures of 9-Vertex Arachno Boron Hydride Clusters. An ab Initio/IGLO/NMR Study

Matthias Hofmann*,[†] and Paul von Ragué Schleyer[†,‡]

Center for Computational Quantum Chemistry, University of Georgia, 1004 Cedar Street,
Athens, Georgia 30602-2525, and Computer-Chemie-Centrum, Institut für Organische Chemie,
Universität Erlangen−Nürnberg, Henkestrasse 42, D-91052 Erlangen, Germany

Received November 18, 1997

The ab initio/IGLO/NMR method clarifies the structures of several 9-vertex boron hydride clusters by comparing computed chemical shifts using various geometries with NMR data in solution. The experimental coordinates of n-B_9H_{15} give an energy 110 kcal mol^{-1} above the fully optimized ab initio geometry. The experimental boron positions were shown to be accurate, but not the hydrogen placements. n-B_9H_{15}, which has a 7-vertex open face binding five bridge hydrogens and one endo terminal H, is 2.2 kcal mol^{-1} lower in energy than the isomer, i-B_9H_{15}. i-B_9H_{15} has a C_{3v} symmetric structure in solution with six asymmetric hydrogen bridges on the open B_6 face of the 9-vertex *arachno* cluster. In contrast to the C_s structure reported for the solid state, $[B_9H_{14}]^-$ is shown to have a fluctional C_1 structure in solution with an additional hydrogen bridge. However, the C_s and C_1 geometries are very similar and the barriers for endo hydrogen rearrangements are 2.4 kcal mol^{-1} or less. $B_9H_{13}{\cdot}NCCH_3$ favors C_1 symmetry in solution in contrast to the reported C_s solid-state structure which has one fewer hydrogen bridge. In contrast to the experimental solid-state structures, in solution $B_9H_{13}{\cdot}NCCH_3$ and $[B_9H_{14}]^-$ are isostructural. A solid-state model for $[B_9H_{13}]^{2-}$ based on the presence of only three instead of five possible structures is proposed. These three structures may also coexist in a fluctuating mixture in solution.

Introduction

The Erlangen ab initio/IGLO[1] (or GIAO)/NMR method[2] has become a powerful tool for structure determination with numerous applications in boron chemistry.[2−10] Comparison of measured chemical shifts with those computed[1] using various geometries showed that the best agreement for a large set of reference molecules and ions was obtained with theoretical rather than experimental structures.[1b] The first application clarified the structures of *arachno*-B_5H_{11} and *arachno*-B_6H_{12}.[3,4] A long-lasting uncertainty was decided in favor of a fluxional C_1 and against a static C_s symmetric B_5H_{11} solution structure.[3] The experimental geometric parameters for B_6H_{12} determined from gas phase electron diffraction were found to be highly inaccurate;[4] the reliability of the ab initio structure was confirmed by subsequent electron diffraction redetermination.[5] The ab initio/IGLO or GIAO/NMR method also has been used extensively more recently to characterize newly synthesized compounds[6] e.g. the *arachno*-2,5-μ-CH_2-1-CB_4H_8 derivatives.[7] Computed ^{11}B NMR chemical shifts have also been applied to check, to refine and even to correct structures which were suggested in the earlier literature.[7b] For example, the widely accepted *closo*-C,3-Me_2-1,2-$C_2B_3H_3$ proposal was shown to be mistaken, recently.[8] Hence, such theoretical studies are especially helpful complements to experiments. Not only do they allow an independent assessment of the accuracy of experimental structure determinations, but also provide insights into structures and dynamic behavior of compounds in solution.[9]

Our recent study of 10-vertex arachno and hypho boron hydrides[10] determined the structures of $[B_{10}H_{13}]^-$ (C_1, fluxional) and $[B_{10}H_{12}]^{2-}$ (C_2, fluxional) in solution. The formation of

---

[†] University of Georgia.

[‡] Universität Erlangen−Nürnberg.

(1) IGLO: (a) Kutzelnigg, W. *Israel. J. Chem.* **1980**, *19*, 193. (b) Schindler, M.; Kutzelnigg, W. *J. Chem. Phys.* **1982**, *76*, 1919. (c) Kutzelnigg, W.; Fleischer, U.; Schindler, M. *NMR: Basic Princ. Prog.* **1990**, *23*, 165.

(2) (a) Bühl, M. In *Encyclopedia of Computational Chemistry*; Schleyer, P. v. R. (Ed. in Chief); Wiley: New York, 1998. (b) Bühl, M.; Schleyer, P. v. R. *J. Am. Chem. Soc.* **1992**, *114*, 477. (c) Bühl, M.; Gauss, J.; Hofmann, M.; Schleyer, P. v. R. *J. Am. Chem. Soc.* **1993**, *115*, 12385. (d) Bühl, M.; Schleyer, P. v. R.; McKee, M. L. *Heteroatom. Chem.* **1991**, *2*, 499. (e) Bühl, M.; Schleyer, P. v. R.; Havlas, Z.; Hnyk, D.; Hermanek, S. *Inorg. Chem.* **1991**, *30*, 3107. (f) Köster, R.; Seidel, G.; Wrackmeyer, B.; Blaeser, D.; Boese, R.; Bühl, M.; Schleyer, P. v. R. *Chem. Ber.* **1992**, *125*, 663; **1991**, *124*, 2715. (g) Bausch, J. W.; Prakash, G. K. S.; Bühl, M.; Schleyer, P. v. R.; Williams, R. E. *Inorg. Chem.* **1992**, *31*, 3060. (h) Bühl, M.; Mebel, A. M.; Charkin, O. P.; Schleyer, P. v. R. *Inorg. Chem.* **1992**, *31*, 3769. (i) Mebel, A. M.; Charkin, O. P.; Bühl, M.; Schleyer, P. v. R. *Inorg. Chem.* **1993**, *32*, 463. (j) McKee, M. L.; Bühl, M.; Schleyer, P. v. R. *Inorg. Chem.* **1993**, *32*, 1712. (k) Hnyk, D.; Brain, P. T.; Rankin, D. W. H.; Robertson, H. E.; Greatrex, R.; Greenwood, N. N.; Kirk, M.; Bühl, M.; Schleyer, P. v. R. *Inorg. Chem.* **1994**, *33*, 2572. (l) Brain, P. T.; Rankin, D. W. H.; Robertson, H. E.; Alberts, I. L.; Hofmann, M.; Schleyer, P. v. R. *Inorg. Chem.* **1994**, *33*, 2565. (m) Hnyk, D.; Rankin, D. W. H.; Robertson, H. E.; Hofmann, M.; Schleyer, P. v. R.; Bühl, M. *Inorg. Chem.* **1994**, *33*, 4781. (n) Hnyk, D.; Brain, P. T.; Robertson, H. E.; Rankin, D. W. H.; Hofmann, M.; Schleyer, P. v. R.; Bühl, M. *J. Chem. Soc., Dalton Trans.* **1994**, 2885. (o) Brain, P. T.; Rankin, D. W. H.; Robertson, H. E.; Alberts, I. L.; Downs, A. J.; Greene, T. M.; Hofmann, M.; Schleyer, P. v. R. *J. Chem. Soc., Dalton Trans.* **1995**, 2193. (p) Hnyk, D.; Hofmann, M.; Schleyer, P. v. R.; Bühl, M.; Rankin, D. W. H. *J. Phys. Chem.* **1996**, *100*, 3435. (q) Brain, P. T.; Cowie, J.; Donohoe, D. J.; Hnyk, D.; Rankin, D. W. H.; Reed, D.; Reid, B. D.; Robertson, H. E.; Welch, A. J.; Hofmann, M.; Schleyer, P. v. R. *Inorg. Chem.* **1996**, *35*, 1701. (r) Compare "the number of successful experimental vs calculational correlations that have now been made strongly suggest that structural assignments based on the ab initio/IGLO/NMR method are quickly approaching a confidence level that rivals modern-day X-ray diffraction determinations of molecular structures," in: Onak, T.; Tseng, J.; Diaz, M.; Tran, D.; Arias, J.; Herrera, S.; Brown, D. *Inorg. Chem.* **1993**, *32*, 487. For extensive bibliographies, see: (s) Onak, T.; Diaz, M.; Barfield, M. *J. Am. Chem. Soc.* **1995**, *117*, 1403. (t) Diaz, M.; Jaballas, J.; Arias, J.; Lee, H.; Onak, T. *J. Am. Chem. Soc.* **1996**, *118*, 4405.

10.1021/ic9714450 CCC: $18.00

adducts with solvent molecules, concluded from experimental findings, could be shown not to be important. Theoretical investigations are particularly favorable adjunct to experiments when highly reactive compounds such as the $[B_{10}H_{12}]^{2-}$ dianion[11] are involved, since instability does not pose any special problems for computations. We now apply the ab initio/IGLO/NMR method to examine the solid state and solution structures of the $[B_9H_{13}]^{2-}$ dianion and other 9-vertex arachno boron hydrides, i.e., *n*-B_9H_{15}[12] and its isomer, *i*-B_9H_{15},[13] as well as $[B_9H_{14}]^-$ [14] and $B_9H_{13}{\cdot}L$.[15] The results differ significantly from the experimental findings for all these species.

Computational Details

Structures usually were optimized consecutively at the HF/3-21G, HF/6-31G*, and MP2(fc)/6-31G* levels of theory[16] using the Gaussian 94 program package.[17] Unless noted otherwise, only the MP2 geometries are reported. Analytical frequency calculations at HF levels establish the nature of the stationary points. Relative MP2(fc)/6-31G* energies were corrected for scaled (0.89) differences in zero point vibrational energies (HF/6-31G*). Chemical shifts were computed with the IGLO method[1,18] using Huzinaga DZ basis sets[19] in the recommended contraction scheme: 3s [21] for H and 7s3p [4111,21] for B. B_2H_6 ($\sigma = 114.88$) served as a primary reference for computed ^{11}B chemical shifts; the experimental B_2H_6 gas-phase value, $\delta = 16.6$,[20] was used to convert to the experimental standard, $BF_3{\cdot}OEt_2$. Coupling constants were computed using the density functional aproach[21] implemented in the deMon program.[22] The exchange functional by Perdew and Wang[23] together with the Perdew correlation functional,[24] a radial 64 point grid, the IGLO−III basis set ((11s7p2d) [5111111,211111,11] for B and (6s2p) [3111,11] for H);[18c,19] a perturbation parameter of 0.001 based on the center of the hydrogen atoms was applied.

Results and Discussion

***n*-B_9H_{15}.** Isolated from a discharge reaction from diborane(6) and pentaborane(9),[25] *n*-B_9H_{15} was the first new borane[12] described (over 30 years later) after the seminal work of Stock.[26] The X-ray structure[27] of *n*-B_9H_{15} did not correspond to the *arachno*-9-vertex cluster with an open VI-face (*arachno*-9⟨VI⟩, see Scheme 1) expected from empirical rules,[28] but to the open VII-face alternative (*arachno*-9⟨VII⟩) which results from removing vertex 5 instead of vertex 6 from the *nido*-10 cluster (*nido*-10⟨VI⟩). As the *n*-B_9H_{15} molecules do not lie on an element of symmetry in the crystal (space group $P2_1/n$), the molecular point group from the solid state structure determination is only C_1. However, the deviations from C_s are small suggesting that isolated molecules might have C_s symmetry.

In his interpretive review, “The Molecular Structures of Boranes and Carboranes”,[29] Beaudet recommended geometrical parameters of an averaged C_s symmetric structure of *n*-B_9H_{15} based on the data of ref 27. However, when this recommended geometry is used for a single point computation, the MP2(fc)/6-31G* energy is 110.7 kcal mol^{-1} higher than that computed with full optimization (**1**, Figure 1). The large error is mostly due to the hydrogen atom positions which were not determined accurately in the early X-ray analysis.[30] This is shown by a partial optimization (“H popt”). All the hydrogen parameters were allowed to vary while keeping all the boron atom coordinates fixed. This procedure lowers the relative energy to only 3 kcal mol^{-1} above that of the fully optimized geometry. Although the averaged experimental $B-H^{\mu}$ distances given in Figure 1 appear to be reasonable (e.g. $B4,9-H^{\mu} = 1.31$ Å),

---

(3) Schleyer, P. v. R.; Bühl, M.; Fleischer, U.; Koch, W. *Inorg. Chem.* **1990**, *29*, 153.

(4) Bühl, M.; Schleyer, P. v. R. *Angew. Chem.* **1990**, *102*, 962.

(5) Brain, P. T.; Hnyk, D.; Rankin, D. W. H.; Bühl, M.; Schleyer, P. v. R. *Polyhedron* **1994**, *13*, 1453.

(6) (a) Unverzagt, M.; Subramanian, G.; Hofmann, M.; Schleyer, P. v. R.; Berger, S.; Harms, K.; Massa, W.; Berndt, A. *Angew. Chem.* **1997**, *109*, 1567; *Angew. Chem., Int. Ed. Engl.* **1997**, *36*, 1469. (b) Unverzagt, M.; Winkler, H.-J.; Brock, M.; Hofmann, M.; Schleyer, P. v. R.; Massa, W.; Berndt, A. *Angew. Chem.* **1997**, *109*, 879; *Angew. Chem., Int. Ed. Engl.* **1997**, *36*, 853−855. (c) Bausch, J. W.; Matoka, D. J.; Caroll, P. J.; Sneddon, L. G. *J. Am. Chem. Soc.* **1996**, *118*, 11423.

(7) a) Gangnus, B.; Stock, H.; Siebert, W.; Hofmann, M.; Schleyer, P. v. R. *Angew. Chem.* **1994**, *106*, 2383; *Angew. Chem., Int. Ed. Engl.* **1994**, *33*, 2296. (b) Fox, M. A.; Greatrex, R.; Hofmann, M.; Schleyer, P. v. R. *Angew. Chem.* **1994**, *106*, 2384; *Angew. Chem., Int. Ed. Engl.* **1994**, *33*, 2298.

(8) Hofmann, M.; Fox, M. A.; Greatrex, R.; Schleyer, P. v. R.; Bausch, J. W.; Williams, R. E. *Inorg. Chem.* **1996**, *35*, 6170.

(9) Fox, M. A.; Greatrex, R.; Hofmann, M.; Schleyer, P. v. R.; Williams, R. E. *Angew. Chem.* **1997**, *109*, 1542; *Angew. Chem., Int. Ed. Engl.* **1997**, *36*, 1498.

(10) Hofmann, M.; Schleyer, P. v. R. *Inorg. Chem.* **1998**, *37*, 5557.

(11) Bridges, A. N.; Gaines, D. F. *Inorg. Chem.* **1996**, *34*, 4523.

(12) (a) Eriks, E.; Lipscomb, W. N.; Schaeffer, R. *J. Chem. Phys.* **1954**, *22*, 754. (b) Kotlensky, W. V.; Schaeffer, R. *J. Am. Chem. Soc.* **1958**, *80*, 4517.

(13) Dobson, J.; Keller, P. C.; Schaeffer, R. *J. Am. Chem. Soc.* **1965**, *87*, 3522.

(14) Benjamin, L. E.; Stafiej, S. F.; Takacs, E. A. *J. Am. Chem. Soc.* **1963**, *85*, 2674.

(15) (a) Graybill, B. M.; Pitochelli, A. R.; Hawthorne, M. F. *Inorg. Chem.* **1962**, *1*, 626. (b) Schaeffer, R.; Walter, W. *Inorg. Chem.* **1973**, *12*, 2209. (c) Bodner, G. M.; Scholer, F. R.; Todd, J. L.; Senor, L. E.; Carter, J. C. *Inorg. Chem.* **1971**, *10*, 942.

(16) For an introduction to computational chemistry and the usual nomenclature, see: (a) Foresman, J. B.; Frisch, Æ. *Exploring Chemistry with Electronic Structure Methods: A Guide to Using Gaussian*; Gaussian Inc.: Pittsburgh, PA, 1993. (b) Hehre, W. J.; Radom, L.; Schleyer, P. v. R.; Pople, J. A. *Ab Initio Molecular Orbital Theory*; Wiley: New York, 1986.

(17) Frisch, M. J.; Trucks, G. W.; Schlegel, H. B.; Gill, P. M. W.; Johnson, B. G.; Robb, M. A. Cheeseman, J. R.; Keith, T.; Petersson, G. A.; Montgomery, J. A.; Raghavachari, K.; Al-Laham, M. A.; Zakrzewski, V. G.; Ortiz, J. V.; Foresman, J. B.; Cioslowski, J.; Stefanov, B. B.; Nanayakkara, A.; Challacombe, M.; Peng, C. Y.; Ayala, P. Y.; Chen, W.; Wong, M. W.; Andres, J. L.; Replogle, E. S.; Gomperts, R.; Martin, R. L.; Fox, D. J.; Binkley, J. S.; Defrees, D. J.; Baker, J.; Stewart, J. P.; Head-Gordon, M.; Gonzalez, C.; Pople, J. A. *Gaussian 94*, Revision C.3; Gaussian, Inc.: Pittsburgh, PA, 1995.

(18) GIAO and other methods implemented, e.g. in the Gaussian program,[17] can be employed similarly.

(19) Huzinaga, S. *Approximate Atomic Wave Functions*; University of Alberta: Edmonton, 1971.

(20) Onak, T. P.; Landesman, H. L.; Williams, R. E. *J. Phys. Chem.* **1959**, *63*, 1533.

(21) Malkin, V. G.; Malkina, O. L.; Salahub, D. R. *Chem. Phys. Lett.* **1994**, *221*, 91.

(22) (a) St-Amant, A.; Salahub, D. R. *Chem. Phys. Lett.* **1990**, *169*, 387. (b) Salahub, D. R.; Fournier, R.; Mlynarski, P.; Papai, I.; St-Amand, A.; Ushio, J. in *Density Functional Methods in Chemistry*; Labanowski, K. J., Andzelm, J. W., Eds.; Springer: Berlin, 1991; p 77. (c) Godbout, N.; Salahub, D. R.; Wimmer, E. *Can. J. Chem.* **1992**, *70*, 560.

(23) Perdew, J. P.; Wang, Y. *Phys. Rev. B* **1986**, *33*, 8800.

(24) Perdew, J. P. *Phys. Rev. B*, **1986**, *33*, 8822, 7406.

(25) Ditter, J. F.; Spielman, J.; Williams, R. E. *Inorg. Chem.* **1966**, *5*, 118.

(26) Stock, A. *Hydrides of Boron and Silicon*; Cornell University Press: Ithaca, NY, 1933 and 1957.

(27) (a) Dickerson, R. E.; Wheatley, P. J.; Howell, P. A.; Lipscomb, W. N. *J. Chem. Phys.*, **1957**, *27*, 200. (b) Simpson, P. G.; Lipscomb, W. N. *J. Chem. Phys.* **1961**, *35*, 1340.

(28) Williams, R. E. *Chem. Rev.* **1992**, *92*, 177.

(29) Beaudet, A. In *Advances in Boron and the Boranes*; Liebman, J. F., Greenberg, A., Williams, R. E., Eds.; VCH: Weinheim, 1988; Chapter 20, p 417.

(30) There appears to be an error in the Cartesian coordinates for the averaged structure. While the distance B6−B7 is given as 1.78 Å in agreement with the original work, a value of 1.86 Å is derived from the Cartesian coordinates. However, this large difference results in only a small additional energetic effect. The original coordinates (C_1 symmetry) give a relative energy of 111.2 kcal mol^{-1} relative to the fully optimized geometry.

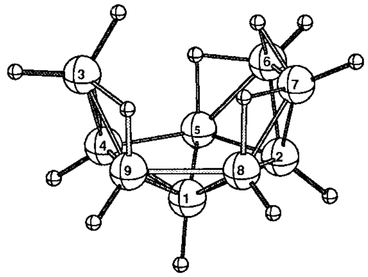

1, C_s

	//MP2(fc)/6-31G*	exp.
B1-B2	1.775	1.77
B1-B4	1.743	1.76
B1-B5	1.739	1.75
B2-B5	1.808	1.82
B2-B6	1.732	1.78
B3-B4	1.845	1.86
B4-B5	1.931	1.95
B4-B9	1.776	1.80
B5-B6	1.788	1.84
B6-B7	1.756	1.78
B3-H^{μ}	1.403	1.46
B4-H^{μ}	1.257	1.31
B5-H^{μ}	1.326	1.33
B6-$H^{\mu(B5)}$	1.319	1.24
B3-$H^{\mu(B6)}$	1.340	1.41

Figure 1. The C_s symmetry molecular structure of *n*-B_9H_{15}, **1**, optimized at MP2(fc)/6-31G*, compared with the best experimental data (ref 29, averaged from the C_1 X-ray crystal structure of ref 27).

Table 1. ^{11}B NMR Chemical Shifts [ppm] Computed for Various *n*-B_9H_{15} (**1**) Geometries Compared to Measured Data

	B1	B2	B3	B4, B9	B5, B8	B6, B7
//expt[a]	22.7	−46.7	−1.9	−28.2	0.5	6.0
//expt[b]	27.2	−43.7	3.3	−42.9, −10.9	13.1, 1.6	10.5, 3.3
//expt,[b] av	27.2	−43.7	3.3	−26.9	7.4	6.9
//Hpopt,[c]	19.0	−50.2	4.4	−33.1, −34.5	6.5, 7.6	7.6, 12.5
//Hpopt,[c] av	19.0	−50.2	4.4	−33.8	7.1	10.1
//MP2(fc)/6-31G*	19.3	−51.3	2.4	−34.2	3.3	7.6
experiment[d]	*17.2*	*−47.5*	*3.5*	*−32.0*	*3.3* [f]	*7.1* [f]
experiment[e]	*15.9*	*−46.0*	–	*−32.0*	*2.7* [f]	*6.6* [f]

[a] Averaged (C_s) experimental geometry, taken from ref 29. [b] Experimental geometry (C_1) taken from ref 27. [c] Heavy atom coordinates according to experimental geometry in ref 27, hydrogen positions optimized at MP2(fc)/6-31G*. [d] Reference 31. [e] Reference 32. [f] Experimentally, B5,8 and B6,7 could not be assigned.

some of the individual experimental values differed substantially; for example B4−H^{μ} (1.07 Å) and B9−H^{μ} (1.55 Å). The former value is even shorter than some of the terminal B−H distances.

The ^{11}B NMR chemical shifts for *n*-B_9H_{15}, computed and measured,[31,32] are compared in Table 1. The $\delta^{11}B = 3.3$ and 7.1[31] (2.7 and 6.6 in ref 32) signals could not be assigned unequivocally experimentally, but these are differentiated by the theoretical data: B5,8 ($\delta = 3.3$) and B6,7 ($\delta = 7.6$). The agreement between the experimental ^{11}B shifts and the values computed using Beaudet's averaged experimental C_s structure is worse but the discrepancies (the maximum deviation is 6.3 ppm for B1) are not as serious as one might expect in view of the large error in the energy due to the poor hydrogen placements (see above).

The computed ^{11}B chemical shifts of individual boron atoms (of pairs which become identical in C_s symmetry) differ considerably for the experimental C_1 geometry, but their average is relatively close to the experimental NMR values. The large C_1 $\delta^{11}B$ differences are due to the inaccurate H positions. The H-optimized geometry ("H popt") gives boron shifts much closer to each other and their average compares with experimental data as well as those of the fully optimized structure.

***i*-B_9H_{15}.** Protonation of the $[B_9H_{14}]^-$ anion results in the thermally unstable *n*-B_9H_{15} isomer known as "*i*-B_9H_{15}".[13] At temperatures above −35 °C this isomer loses H_2 and forms B_8H_{12}, $B_{10}H_{14}$, and *n*-$B_{18}H_{22}$ or, in the presence of Lewis bases L, gives B_9H_{13}•L adducts.[33] As in $[B_9H_{14}]^-$, the boron atoms are expected to comprise a cluster with an open VI-face (Scheme 1), typical for nine vertex arachno compounds. However, the exact positions of the six extra hydrogens are not known. The experimental ^{11}B NMR spectrum is simple: three doublets, suggesting C_{3v} symmetry (see **2** in Figure 2).[13,34] Moody and Schaeffer redetermined the ^{1}H and ^{11}B NMR spectra and agreed with the earlier C_{3v} proposal.[35] However, they concede that the possible rapid exchange of three bridge and three terminal hydrogens (instead of six equivalent bridging H's in the C_{3v} geometry) could not be excluded. In particular, it was questioned whether six hydrogen bridges could be accommodated on an open B_6 face, since this might be unfavorable sterically.[35] Perhaps in view of these considerations, Hermánek's review depicted a C_3 structure with three BH_2 groups and three H bridges, **3**,[36] which also would be consistent with the experimental observation of only three ^{11}B signals with equal intensity.

Scheme 1

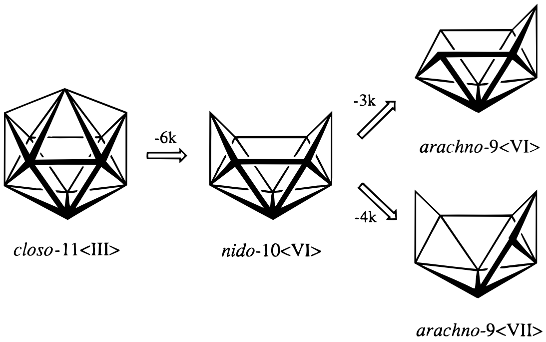

In addition to the earlier *i*-B_9H_{15} proposals, **2** (C_{3v}) and **3** (C_3), we also computed structure **4**, which might result from protonating the B6−B7 edge of the $[B_9H_{14}]^-$ minimum (**7**, see below). A stationary point could be located for **3** only at the HF/3-21G level; moreover, this had three imaginary frequencies (227i cm^{-1} E, 142i cm^{-1} A_2). At HF/6-31G*, a starting geometry based on **3** converged to minimum **2**. A C_1 input geometry for **4** optimizes to a C_s minimum at HF/3-21G and also at HF/6-31G*. Relative energies at MP2(fc)/6-31G* are 0.0, 12.7, and 0.8 kcal mol^{-1} for **2**, **3**, and **4**, respectively. While **2** and **4** could be optimized at MP2(fc)/6-31G*, the value for **3** (a stationary point only at HF/3-21G), is based on an MP2(fc)/6-31G*//HF/3-21G single point energy calculation.

Computed ^{11}B chemical shifts are compared to experimental results in Table 2. The very large deviation for **3** reflects its high relative energy and the fact that **3** is not a stationary point at higher levels of theory. Since **4** is very close in energy to **2**, rapid interchange of endo and bridge hydrogens might give the experimentally observed peaks. However, this is not the case: averaging the computed chemical shifts for **4** results in large differences from the observed NMR data. Hence, both **3** and **4** are ruled out as structural candidates. In contrast, the C_{3v} symmetric structure **2** shows satisfactory agreement with the measured chemical shifts. This confirmation of **2** as the *i*-B_9H_{15} solution structure demonstrates that six hydrogen bridges can be accommodated on an open B_6-face. Note that the hydrogen bridges are quite asymmetric. Computed B−H^{μ} distances are 1.255 and 1.474 Å for B4,6,8 and B5,7,9, respectively. Typical B−H^{μ} distances are around 1.30−1.35 Å. Moody and Schaeffer

---

[31] Allerhand, A.; Clouse, A. O.; Rietz, R. R., Roseberry, T.; Schaeffer, R. *J. Am. Chem. Soc.* **1972**, *94*, 2445.
[32] Schaeffer, R.; Sneddon, L. G. *Inorg. Chem.* **1972**, *11*, 3102.
[33] Dobson, J.; Keller, P. C.; Schaeffer, R. *Inorg. Chem.* **1968**, *7*, 399.
[34] Keller, P. C. *Inorg. Chem.* **1970**, *9*, 75.
[35] Moody, D. C.; Schaeffer, R. *Inorg. Chem.* **1976**, *15*, 233.
[36] Hermánek, S. *Chem. Rev.* **1992**, *92*, 325.

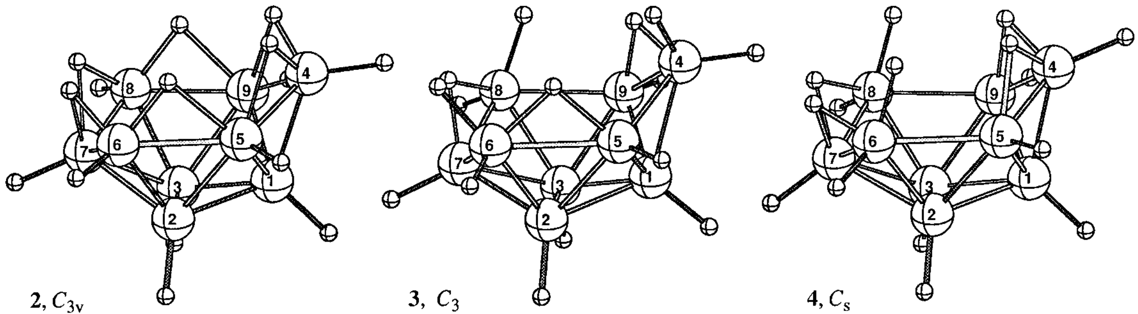

2, C_{3v}
$E_{rel} = 0.0$ kcal mol^{-1}
MIN

3, C_3
$E_{rel} = 12.7$ kcal mol^{-1}

4, C_s
$E_{rel} = 0.8$ kcal mol^{-1}
MIN

B1-B2	1.751
B1-B4	1.818
B1-B9	1.726
B4-B5	1.839
B4-H^{μ}	1.255
B5-H^{μ}	1.474

//RHF/3-21G

B1-B2	1.782	B4-H^{μ}	1.324
B1-B4	1.740	B5-H^{μ}	1.305
B1-B9	1.808	B4-H^{exo}	1.181
B4-B5	1.913	B4-H^{endo}	1.205
B4-B9	1.953		

B1-B2	1.755	B5-B6	1.906
B1-B4	1.727	B6-B7	1.913
B1-B5	1.794	B4-H^{μ}	1.281
B2-B3	1.749	B5-H^{μ}	1.375
B2-B5	1.746	B6-H^{μ}	1.300
B2-B6	1.772	B7-H^{μ}	1.350
B4-B5	1.798		

Figure 2. Optimized geometries of *i*-B_9H_{15} candidate structures **2**, **4** (//MP2(fc)/6-31G*), and **3** (//HF/3-21G*). (The 3-fold symmetry axes of **2** and **3** pass through the centers of the B1−B2−B3, as well as the B4−B6−B8 and B5−B7−B9 triangles.)

Table 2. IGLO/DZ Computed Chemical Shifts [ppm] for *i*-B_9H_{15} Structures **2**, **3**, and **4** Compared to Experiment

	B1, B2,3	B4, B6,8	B5,9, B7
2, C_{3v}	−38.6	−47.3	4.6
3, C_3[a]	−16.8	27.6	−29.6
4, C_s	−49.0, −7.8	−16.7, −41.3	23.2, −16.9
4, C_s, av	−21.5	−33.1	23.5
experiment[b]	*−32.9*	*−44.8*	*4.39*

[a] At the HF/3-21G geometry. [b] Reference 35.

Table 3. Experimental and Theoretical[a] $^{11}B-^{1}H$ Coupling Constants [Hz] for *i*-B_9H_{15}

	B4,6,8-H^{μ}	B5,7,9-H^{μ}
2[b]	51.9	26.5
3[c]	64.4[d]	22.0
experiment[e]	*50*	*25−35*

[a] SOS-IGLO/PW86/III. [b] //MP2(fc)/6-31G*. [c] //HF/3-21G. [d] Average value assuming rapid interconversion of bridge and endo terminal hydrogens; individual values are 90.7 (B−H^{endo}) and 38.2 (B−H^{μ}). [e] Reference 35.

deduced "a slight asymmetry of the bridges", toward B4,6,8 and away from B5,7,9, from the observed large $J_{^{11}B-^{1}H}$ coupling of 50 Hz between B4,6,8 and bridging hydrogens.[35] They also gave a rough estimate of 25−35 Hz for the B5,7,9-H^{μ} coupling. These $J_{^{11}B-^{1}H}$ values are reproduced computationally for structure **2** quite well: 51.9 and 26.5 Hz, respectively (Table 3). For **3**, however, we compute 90.7 (B4−H^{endo}), 38.2 (B4−H^{μ}), −6.9 (B5−$H^{endo,B4}$) and 50.9 Hz (B5−H^{μ}). Averaging (assuming a rapid interconversion of bridge and endo terminal H's in **3**) gives 64.4 (B4−H) and 22.0 Hz (B5−H). Like $\delta^{11}B$, these values also do not agree well with the experimental data either. Hence, comparison of computed and measured $\delta^{11}B$ chemical shifts and $J_{^{11}B-^{1}H}$ coupling constants (compare Table 3) favor structure **2** over **3**.

i-B_9H_{15} is one of the rare cases where more than one boron hydride isomer is known experimentally. Williams wrote "appraisal suggests that the six skeletal hydrogens in the aberrant *n*-B_9H_{15} structure are considerably more stable than in *i*-B_9H_{15}".[28] While *i*-B_9H_{15} decomposes more easily, and thus has a higher reactivity, it is almost as stable as *n*-B_9H_{15} thermodynamically. The computed relative energy of *i*-B_9H_{15} is only 2.2 kcal mol^{-1} higher.

$[B_9H_{14}]^-$. *arachno*-$[B_9H_{14}]^-$ was first obtained by Benjamin et al. in 1963 from the basic degradation of $B_{10}H_{14}$ in H_2O.[14] As $[B_9H_{14}]^-$ could be transformed into $B_9H_{13}{\cdot}NMe_3$, the anion was postulated to have a structure similar to $B_9H_{13}{\cdot}NCMe$, for which an X-ray structure was known.[37] The $[B_9H_{14}]^-$ cluster belongs to the *arachno*-9-⟨VI⟩ category (see Scheme 1). Both B5/B6 and B8/B9 are hydrogen bridged while B4, B6, and B8 have additional endo H's (**5**, Figure 3). In $B_9H_{13}{\cdot}L$, the exo terminal H at B4 is replaced by L.

Keller's subsequent ^{11}B NMR spectrum did not support a static $[B_9H_{14}]^-$ solution structure with an endo hydrogen arrangement analogous to the $B_9H_{13}{\cdot}NCMe$ X-ray: the three different boron signals of equal intensity each show only one kind of coupling to ^1H.[34] Keller's success in exchanging five hydrogens by deuterium suggested that there were five bridging H's. ^{11}B NMR chemical shifts, not given by Keller, have only been published by Greenwood et al. who also were able to determine the X-ray structure of $[B_9H_{14}]^-$ in the Cs salt.[38] The three BH_2 moieties found in the solid state are not arranged like those in $B_9H_{13}{\cdot}NCMe$. Instead, B4 shares hydrogen bridges with B5,9; in addition, B7 and B6,8 have terminal hydrogens (**6**). Greenwood et al. speculated that fluctuation in solution is responsible for the effective C_{3v} symmetry on the NMR time scale. However, the possibility of five hydrogen bridges in solution could not be excluded. Jacobson et al. finally compared various neutral and anionic $B_9H_{13}{\cdot}L$ compounds and assigned ^{11}B signals based on isotope labeling experiments.[39]

Structure **6**, determined to have C_s symmetry in the solid state,[38] is characterized as a transition structure (457i cm^{-1}) by HF/6-31G* computations (which pertain to the gas phase). Optimization without symmetry restrictions converged to the C_1 minimum, **7** (Figure 3). This has an additional H bridge between B7/B8 and is 2.3 kcal mol^{-1} more stable than **6** (which

---

(37) Wang, F. E.; Simpson, P. G.; Lipscomb, W. N. *J. Chem. Phys.* **1961**, *35*, 1335.

(38) (a) Greenwood, N. N.; Gysling, H. J.; McGinnety, J. A.; Owen, J. D. *J. Chem. Soc., Chem. Commun.* **1970**, 505. (b) Greenwood, N. N.; Gysling, H. J.; McGinnety, J. A.; Owen, J. D. *J. Chem. Soc., Dalton Trans.* **1972**, 986.

(39) Jacobsen, G. B.; Morris, J. H. *J. Chem. Soc., Dalton Trans.* **1984**, 415.

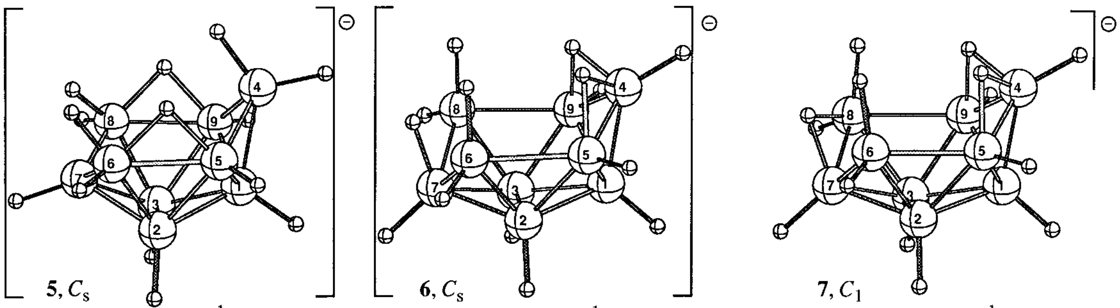

5, C_s
E_{rel} = 2.4 kcal mol^{-1}
TS (411i cm^{-1}, A")

B1-B2	1.780	B4-B5	1.887
B1-B4	1.739	B5-B6	1.834
B1-B5	1.731	B6-B7	1.850
B2-B3	1.793	B5-H^{μ}	1.324
B2-B5	1.790	B6-H^{μ}	1.328
B2-B6	1.721	B6-H^{exo}	1.234
B2-B7	1.774	B6-H^{endo}	1.196

6, C_s
E_{rel} = 2.3 kcal mol^{-1}
TS (457i cm^{-1}, A")

B1-B2	1.800	B4-B5	1.783
B1-B4	1.707	B5-B6	2.005
B1-B5	1.771	B6-B7	1.883
B2-B3	1.803	B4-H^{μ}	1.316
B2-B5	1.726	B5-H^{μ}	1.338
B2-B6	1.750	B6-H^{endo}	1.205
B2-B7	1.748	B7-H^{endo}	1.227

7, C_1
E_{rel} = 0.0 kcal mol^{-1}
MIN

	calc.	exp.		calc.	exp.
B1-B2	1.796	1.790(11)	B1-B3	1.796	1.787(11)
B1-B4	1.706	1.701(14)			
B1-B5	1.794	1.767(14)	B1-B9	1.757	1.780(12)
B2-B3	1.786	1.778(11)			
B2-B5	1.731	1.755(13)	B3-B9	1.734	1.743(12)
B2-B6	1.733	1.773(14)	B3-B8	1.780	1.742(12)
B2-B7	1.728	1.771(12)	B3-B7	1.782	1.726(11)
B4-B5	1.797	1.775(12)	B4-B9	1.778	1.794(13)
B5-B6	1.931	1.989(13)	B8-B9	2.023	1.924(12)
B6-B7	1.881	1.883(14)	B7-B8	1.878	1.855(12)
B4-$H^{\mu(B5)}$	1.329	1.17(4)	B4-$H^{\mu(B9)}$	1.297	1.23(5)
B5-H^{μ}	1.323	1.30(4)	B9-H^{μ}	1.367	1.25(5)
B7-H^{μ}	1.277	1.04(5)			
B8-H^{μ}	1.383	-			

Figure 3. Optimized geometries (//MP2(fc)/6-31G*) of various $[B_9H_{14}]^-$ structures **5**, **6**, and **7**. C_1 X-ray data from ref 38b are given together with **7** for comparison.[43] Note, however, that the experimental structure was described to have no bridging hydrogen between H7 and H8, but an *endo*-H at B7 (like **6**).

is the transition structure for the B7−H^{μ}−B8 to B7−H^{μ}−B6 H-shift). Structure **7** also was obtained when a *i*-B_9H_{15} starting geometry with one bridge proton removed was used for a C_1 optimization. The barrier for endo/bridge hydrogen exchange involving transition structure **5** (411i cm^{-1}) is only 2.4 kcal mol^{-1}. Changing the B4/B9 bridge hydrogen in **7** to a terminal hydrogen bound to B4 leads to **5**. (Note that the atom numbering is different: B9 in **7** becomes B7 in **5**.) Bridging of the endo H at B8 or B6 to B7 in **5** leads to **7** or to its enantiomer, respectively.

We applied the SCRF method to model the influence of a polarizable medium (i.e. in solution and in the crystal) on the structure.[40] SCRF optimization also results in a B7−B8 hydrogen bridge. Crystal packing effects, not considered in the SCRF treatment, are unlikely to be important because the C_1 and the C_s cluster geometries do not deviate significantly. That is, the equivalent B−B distances in **7** (C_1) are almost the same and their averages are very close to the corresponding values in **6** (C_s). The largest difference is 0.1 Å between *d*(B5−B6) (1.931 Å) and *d*(B8−B9) (2.023 Å). All other distances deviate less than 0.03 Å. In particular, the endo (**6**) or bridge character (**7**) of the additional hydrogen at B7 does not change the B6−B7 and B7−B8 separations: these are 1.883 Å in **6** and 1.881 and 1.878 Å in **7**, respectively. Hence, it seems possible that $[B_9H_{14}]^-$ forms three hydrogen bridges in the solid state as well as in solution and in the gas phase. Perhaps this was not recognized in the X-ray structure analysis because the C_1 cluster geometry, despite its additional H bridge, deviates very little from C_s symmetry. Furthermore, the two enantiomers should be distributed equally over the positions in the lattice. Determination of the proton positions by X-ray diffraction was not possible. Getman et al.[41] mention that a second, low-temperature structure of $[B_9H_{14}]^-$ which shows a B6/B7 hydrogen bridge[42] was determined at −174 °C. Besides this additional H bridge, the low-temperature structure is in line with the findings at room temperature.[38] Unfortunately, details are not available to us. Coordinates of the high-temperature structure have been published[38] and the fixed boron positions were used as input for a partial hydrogen parameter optimization.[43] As this has to be carried out in C_1 symmetry (the salt crystallizes in space group P1), the endo hydrogen at B7 becomes a B7−B8 hydrogen bridge (d(B7−H^{μ}) = 1.376 Å, d(B8−H^{μ}) = 1.283 Å). The energy is only 0.5 kcal mol^{-1} higher than that of the full optimization.

The ab initio/IGLO/NMR method allows the determination of the solution structure of $[B_9H_{14}]^-$. Relatively small changes in geometry (e.g. those between **6** and **7**) can have a large effect on the chemical shifts (compare Table 4). For most of the boron atoms, the differences are more than 10 ppm between **6** and **7**. Only for B1 and B4, which are farthest away from the B7−H/

---

(40) (a) SCRF optimizations employed the 6-31G* basis set and the following parameters: dielectric constant ϵ = 78.1 (modeling water) and a radius of the cavity r = 4.43 Å. This gives d(B7−H^{μ}) = 1.263 Å, d(B8−H^{μ}) = 1.406 Å, d(B6−H^{μ}) = 2.330 Å, d(B6−B7) = 1.920 Å, d(B7−B8) = 1.919 Å. The MP2(fc)/6-31G* single point energy for this geometry is 1.8 kcal mol^{-1} higher than that for the fully MP2 optimized structure. Chemical shifts computed for the SCRF geometry are −50.2 (B1), 10.9 (B2), −25.8 (B3), −3.7 (B4), −9.2 (B5), −18.0 (B6), −32.2 (B7), −13.0 (B8), and 17.6 (B9). Averaging gives −21.7 (B1,2,3), −11.6 (B4,6,8) and −8.0 (B5,7,9). (b) Examples are known whose experimental structure differ considerably in the gas and in the solid phases. These differences are reproduced well by ab initio computations with and without the SCRF procedure; see: Jiao, H.; Schleyer, P. v. R. *J. Am. Chem. Soc.* **1994**, *116*, 7429.

(41) Getman, T. D.; Krause, J. A.; Niendenzu, P. M.; Shore, S. G. *Inorg. Chem.* **1989**, *28*, 1507.

(42) Reference 10 in ref 41: Huffman, J. Report No. 82210, Indiana University Department of Chemistry Molecular Structure Center.

(43) The coordinates in ref 38b appear to have errors and give a B7−H distance of more than 4 Å (it should be 1.04(6) Å according to another table). Computing the energy or chemical shifts for such a geometry does not seem to be useful. The boron coordinates, however, seem to be correct as all B−B distances correspond to the listed values.

Table 4. ^{11}B NMR Chemical Shifts [ppm] for $[B_9H_{14}]^-$ Candidate Structures Together with Available Experimental Data

	B1		B2, B3	B4		B6, B8	B5	B7	B9
5, C_s	4.8		−45.7	−32.7		−30.3	−18.8	22.7	−18.8
5, C_s, av		−28.9			−31.1			−5.0	
6, C_s	−52.3		−5.6	−1.7		−7.2	1.5	−53.4	1.5
6, C_s, av		−21.2			−5.4			−16.8	
7, C_1	−51.8		−25.5, −25.5	−6.3		−23.0, −20.8	−10.2	−33.2	14.8
7, C_1, av		−22.8			−16.7			−9.5	
//expt[a]									
Hpopt	−52.5		8.7, −24.9	−7.0		−25.4, −24.0	−10.5	−33.1	13.8
Hpopt, av		−22.9			−18.8			−9.9	
expt[b]		*−23.69*			*−20.37*			*−8.17*	
expt[c]		*−21.6*			*−19.7*			*−6.6*	
expt[d]		*−22.4*			*−19.2*			*−6.8*	

[a] Fixed boron geometries from the X-ray structural analysis of the Cs salt, ref 38b, but with the hydrogen positions optimized at MP2(fc)/6-31G*.[43] [b] Cs^+ salt in Me_2SO, without assignment, ref 38a. [c] Reference 45. [d] $[NMe_4]^+$ salt in CD_3CN, refs 39 and 44.

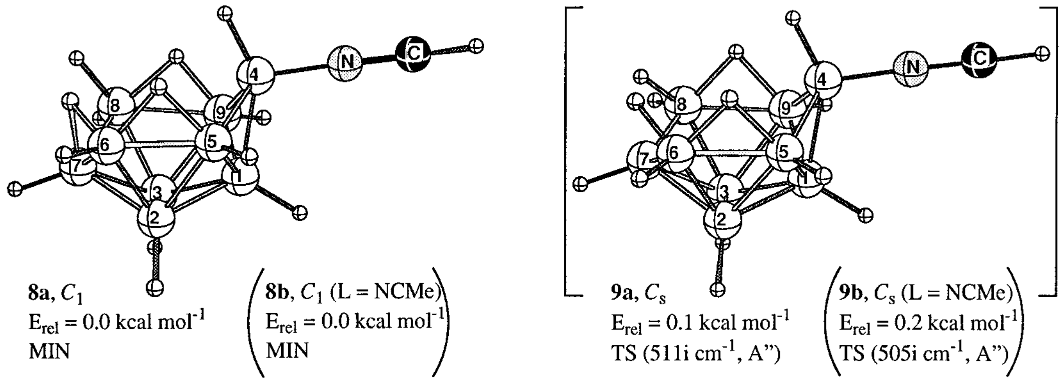

8a, C_1
$E_{rel} = 0.0$ kcal mol^{-1}
MIN

(**8b**, C_1 (L = NCMe)
$E_{rel} = 0.0$ kcal mol^{-1}
MIN)

9a, C_s
$E_{rel} = 0.1$ kcal mol^{-1}
TS (511i cm^{-1}, A”)

(**9b**, C_s (L = NCMe)
$E_{rel} = 0.2$ kcal mol^{-1}
TS (505i cm^{-1}, A”))

B1-B2	1.760 (1.762)	B1-B3	1.750 (1.752)
B1-B4	1.736 (1.735)		
B1-B5	1.751 (1.748)	B1-B9	1.746 (1.745)
B2-B3	1.798 (1.798)		
B2-B5	1.797 (1.797)	B3-B9	1.802 (1.800)
B2-B6	1.714 (1.713)	B3-B8	1.776 (1.776)
B2-B7	1.779 (1.777)	B3-B7	1.742 (1.741)
B4-B5	1.872 (1.876)	B4-B9	1.833 (1.836)
B5-B6	1.804 (1.803)	B8-B9	1.878 (1.878)
B6-B7	1.787 (1.786)	B7-B8	1.969 (1.973)
B5-H^{μ}	1.326 (1.325)	B9-H^{μ}	1.294 (1.292)
B6-$H^{\mu(B5)}$	1.323 (1.325)	B8-H^{μ}	1.352 (1.355)
B6-$H^{\mu(B7)}$	1.284 (1.285)	B7-H^{μ}	1.383 (1.382)
B4-N	1.519 (1.521)	N-C	1.167 (1.169)

	calc.	exp.		calc.	exp.
B1-B2	1.746 (1.748)	1.766	B5-B6	1.824 (1.825)	1.842
B1-B4	1.747 (1.746)	1.731	B6-B7	1.839 (1.839)	1.870
B1-B5	1.751 (1.749)	1.745	B4-N	1.516 (1.519)	1.507
B2-B3	1.798 (1.799)	1.825	N-C	1.168 (1.669)	1.126
B2-B5	1.793 (1.793)	1.785	B5-H^{μ}	1.338 (1.337)	1.21
B2-B6	1.720 (1.719)	1.722	B6-H^{μ}	1.315 (1.316)	1.35
B2-B7	1.806 (1.804)	1.760	B6-H^{endo}	1.242 (1.241)	1.08
B4-B5	1.843 (1.845)	1.865	B7-$H^{endo, B6}$	1.553 (1.558)	

Figure 4. C_1 (**8**) and C_s (**9**) structures (//MP2(fc)/6-31G*) of model compound B_9H_{13}·L, L = HCN (**a**), MeCN (**b**, in parentheses) corresponding to the solution and solid-state structures, respectively. Experimental data refer to B_9H_{13}·NCMe from ref 37.

B7−H^{μ}-B8 site, have smaller differences. Averaged values for **6** and **7**, however, are similar. Nevertheless, **7** can be identified as the correct solution structure since the experimental assignment[39] is followed. For **6**, the B(4,6,8) and B(5,7,9) assignment has to be reversed, and this contradicts the experimental findings.[39] Thus, the computational results show that triply hydrogen bridged **7** (C_1) is the solution structure of $[B_9H_{14}]^-$.

B_9H_{13}·L. Various Lewis base (L) adducts, *arachno*-B_9H_{13}·L, of the still elusive *nido*-B_9H_{13} have been investigated intensively experimentally.[15] These species are obtained from acid-induced degradation of $[B_{10}H_{13}][HL]$ solutions in water or by ligand exchange from B_9H_{13}·SEt_2, which allow the introduction of neutral (L = NH_2Et, $NHEt_2$, NEt_3, PPh_3, NCMe, pyridine)[15] and anionic (NCS^-, $NCSe^-$, $NCBPh_3^-$) ligands.[39,44] The X-ray structure of B_9H_{13}·NCMe in the solid state has been determined.[37] The arachno cluster has an open VI-face (*arachno*-9⟨VI⟩ in Scheme 1). The exo ligand L is bound to B4. Endo hydrogens are bound terminally to B4, B6 as well as B8 and also bridge B5/B6 as well as B8/B9 (C_s symmetry, compare model **9a** in Figure 4).

Model compound B_9H_{13}·NCH is a transition structure at HF/6-31G* in C_s symmetry (**9a**) connecting two degenerate C_1 symmetric minima, **8a**. In **8a**, there is an additional hydrogen bridge between B6/B7 instead of an endo terminal H (as in **9a**). This feature lowers the energy by only 0.1 kcal mol^{-1}. While such a tiny energy difference between **9a** and **8a** does not allow a definitive decision, the computed chemical shifts show clearly that a C_1 (**8**) and not a C_s structure (**9**) is present in solution. As the chemistry of HCN and MeCN is very different, a referee doubted the validity of our results on models **8a** and **9a**. We therefore repeated the computations with L = MeCN (**8b** and **9b**) but the optimized geometries, relative energies (Figure 4), and chemical shifts (Table 5) are almost identical. The maximum difference in chemical shifts (1.6 ppm) between **8a**/**8b** and

---

(44) Meina, D. J.; Morris, J. H. *J. Chem. Soc., Dalton Trans.* **1985**, 1903.
(45) Schaeffer, R.; Sneddon, L. G. *Inorg. Chem.*, **1972**, *11*, 3102.

Table 5. Experimental (L = NCMe) ^{11}B NMR Chemical Shifts [ppm] for B_9H_{13}·L in Comparison to Computed Values[a] for C_1 (**8**) and C_s (**9**) Structures (**a**, L = NCH; **b**, L = NCMe)

	B1	B2, B3	B4	B5, B9	B6, B8	B7
8a, C_1 calcd	11.0	−51.6, −27.2	−29.0	−8.1, −23.6	−9.9, −26.1	21.6
8b, C_1 calcd	11.2	−51.8, −27.2	−27.4	−9.5, −24.7	−9.5, −25.6	21.2
8a, C_1 calcd, av[b]	11.0	−39.4	−29.0	−15.9	−18.0	21.6
8b, C_1 calcd, av[b]	11.2	−39.5	−27.4	−17.1	−17.6	21.2
9a, C_s calcd	4.6	−47.5	−33.3	−13.3	−31.9	16.2
9b, C_s calcd	5.1	−47.6	−31.7	−13.9	−31.7	16.6
B_9H_{13}·NCMe, experiment[c]	*5.6*	*−38.3*	*−27.0*	*−14.0*	*−20.2*	*17.7*

[a] IGLO/DZ//RMP2(fc)/6-31G*. [b] Averaged to C_s symmetry supposing a rapid degenerate rearrangement of **8** through transition state **9**. [c] B_9H_{13}·NCMe in CD_3CN, ref 39.

between **9a**/**9b** is found for B4 which is directly bound to the ligand L. The conclusions remain the same. Again, only the averaged shifts of the C_1 structure (**8b**) are in satisfactory agreement with experimental data (the maximum difference is 5.6 ppm for B1, Table 5). C_s symmetric **9b** shows discrepancies up to 11.5 ppm (B6,8). This strongly suggests a C_1 solution structure for B_9H_{13}·NCMe.

The *arachno*-$[B_9H_{14}]^-$ anion can also be considered to be an *arachno*-B_9H_{13}·L compound with a hydride ion as Lewis base L. Hence, both are expected to be isostructural. However, the experimental solid-state structures of $Cs[B_9H_{14}]$[38] and B_9H_{13}·NCMe[37] are different. The underlying B_9 cluster is the same, but $[B_9H_{14}]^-$ has two geminal hydrogen bridges (between B4/B5 and B4/B9) together with three endo terminal H's at B6,8 and B7 (**6** in Figure 3). In contrast, B_9H_{13}·NCMe shows two separated bridge hydrogens (between B5/B6 and B8/B9), endo terminal H's at B4 as well as B6,8 and a boron atom B7 neither participating in a hydrogen bridge nor carrying an endo terminal hydrogen. Our ab initio/IGLO/NMR results reveal that different structures analogous to each other are favored in solution. Replacing the L (HCN) in **8a** by H^- gives the lowest energy $[B_9H_{14}]^-$ structure, **7**, directly. (Note the change in numbering: B4 in **8a** is labeled B6 in **7** and vice versa.) The only difference in solution is that an exo terminal ligand L seems to prevent the geminal endo terminal hydrogen atom from bridging. Thus, on the NMR time scale, B_9H_{13}·L appears to have C_s while $[B_9H_{14}]^-$ seems to have C_{3v} symmetry.

$[B_9H_{13}]^{2-}$. *arachno*-$[B_9H_{13}]^{2-}$ may be obtained from deprotonating $[B_9H_{14}]^-$ e.g. by $NaNH_2$ in liquid ammonia.[41] An X-ray structure and NMR data have been reported, but the experimental work was discontinued because of explosions when handling $Na[B_9H_{14}]$ and $Na_2[B_9H_{13}]$.[41] This invites computational investigations which do not have such practical problems.

Experimental structural investigations revealed a B_9 cluster for $[B_9H_{13}]^{2-}$ analogous to *i*-B_9H_{15} and $[B_9H_{14}]^-$. However, the four endo hydrogen atoms are disordered and were postulated to occupy five positions (each with an equal probability of 0.8): endo terminal positions at B6, B7 and B8 and two bridge positions between B4/B5 and B4/B9.[41] In solution, all four endo H's fluctuate and there are only three $\delta(^{11}B)$ signals. In the solid state, five structures should be present according to this model. They can be derived from **X** (see Figure 5) by leaving each one of the five endo H positions blank: **X-45** (no H bridge between B4/B5), **X-6** (no endo terminal H at B6), **X-7**, **X-8**, and **X-49**. Relative energies from single point calculations and from hydrogen parameter optimizations, listed in Table 6 for all these possibilities, do not agree with the "five structure" model. The single point results (based on the experimental boron skeleton geometry) show large differences in the relative energies. When the H positions in **X-45** and **X-49** are optimized, the endo terminal H at B7 bridges to B6. The resulting energies are somewhat lower than **X-7** (−1.8 and −1.5 kcal mol^{-1}, respectively). Structures **X-6** and **X-8** do not survive optimizations of the hydrogen positions, and converge to the same **X-7** geometry. The assumption of "five equally populated structures" is not supported. An alternative suggestion seems more realistic. Our model has two endo terminal H's at B6 and B8 together with two endo hydrogen atoms disordered over the four possible bridge positions between B4/B5,9 and B7/B6,8 (i.e. **10**, **11** and **12** also postulated to be also present in solution, see below).

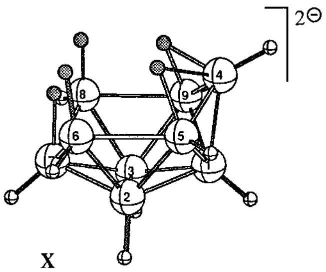

B1-B2	1.716	B1-B3	1.776
B1-B4	1.718		
B1-B5	1.792	B1-B9	1.757
B2-B3	1.773		
B2-B5	1.753	B3-B9	1.756
B2-B6	1.726	B3-B8	1.749
B2-B7	1.754	B3-B7	1.759
B4-B5	1.756	B4-B9	1.762
B5-B6	1.944	B8-B9	1.977
B6-B7	1.847	B7-B8	1.881
B4-$H^{\mu(B5)}$	1.559	B4-$H^{\mu(B9)}$	1.475
B5-H^{μ}	1.311	B9-H^{μ}	1.318
B6-H^{endo}	1.174	B8-H^{endo}	1.125
B7-H^{endo}	1.282		

Figure 5. Experimental solid-state structure, **X**, of the $[B_9H_{13}]^{2-}$ dianion according to Getman et al.[41] Four of the five endo hydrogen positions (identified by dark labels) are occupied and the five possible structures are postulated to be equally weighted.

Table 6. Relative Energies[a] for Various $[B_9H_{13}]^{2-}$ Geometries Postulated to be Present in the Solid State

	X-45	X-6	X-7	X-8	X-49
//expt	8.2	45.2	0.0[b]	45.1	13.3
//H popt[c]	−1.8	–[d]	0.0[e]	–[d]	−1.5

[a] In kcal mol^{-1} at MP2(fc)/6-31G*. [b] The energy of **X-7** relative to **11** is 56.8 kcal mol^{-1}. [c] Hydrogen position optimized for fixed heavy atom coordinates from the X-ray structure (ref 41). [d] **X-6** and **X-8** converge to **X-7** upon optimization of hydrogen parameters. [e] The energy of **X-7** relative to **11** is 6.0 kcal mol^{-1}.

Three geometries starting with the X-ray coordinates have been optimized fully: **10** (corresponding to **X-7**), **11** (corresponding to **X-45**), and **12** (corresponding to **X-49**; Figure 6). Both in **11** and in **12**, the endo H attached to B7 bridges to B8. The relative energies are very close: 1.3, 0.0, and 0.1 kcal mol^{-1} for **10**, **11** and **12**, respectively. Structure **13** with two geminal hydrogen bridges at B7 (B6/B7 and B7/B8) also is a minimum, but much higher in energy (E_{rel} = 34.4 kcal mol^{-1}). A C_s starting geometry with endo terminal hydrogen atoms at B4 and B7 and with hydrogen bridged B5/B6 and B8/B9 converged to **14** which has four endo terminal H's (at B4, B6,8 and B7). Structure **14** is a second-order stationary point (713i A″, 418i cm^{-1} A″) 7.7 kcal mol^{-1} higher in energy than **11**. Optimization of **14** in C_1 symmetry converged to **11**.

Individual and averaged ^{11}B NMR chemical shifts computed for **10** to **14** are compared to experimental data in Table 7. The

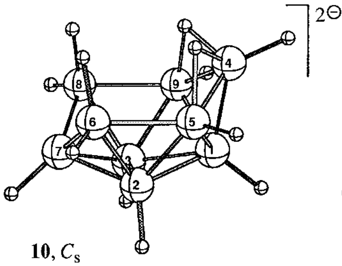

10, C_s
E_{rel} = 1.3 kcal mol^{-1}
MIN

B1-B2	1.810	B4-B5	1.831
B1-B4	1.692	B5-B6	1.889
B1-B5	1.802	B6-B7	1.848
B2-B3	1.756	B4-H^{μ}	1.302
B2-B5	1.753	B5-H^{μ}	1.378
B2-B6	1.754	B6-H^{endo}	1.202
B2-B7	1.732		

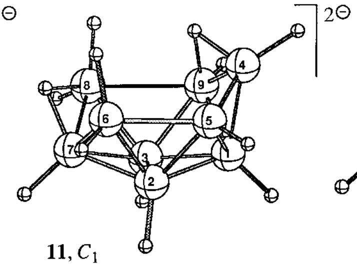

11, C_1
E_{rel} = 0.0 kcal mol^{-1}
MIN

B1-B2	1.765	B3-B9	1.763
B1-B3	1.794	B4-B5	1.675
B1-B4	1.745	B4-B9	1.766
B1-B5	1.818	B5-B6	1.924
B1-B9	1.723	B6-B7	1.877
B2-B3	1.822	B7-B8	1.869
B2-B5	1.739	B8-B9	2.186
B2-B6	1.748	B4-H^{μ}	1.311
B2-B7	1.765	B9-H^{μ}	1.349
B3-B7	1.790	B7-H^{μ}	1.277
B3-B8	1.779	B8-H^{μ}	1.390

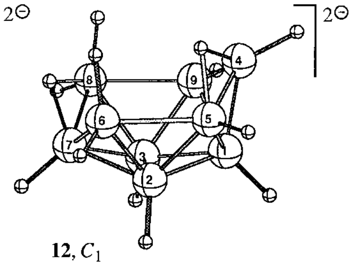

12, C_1
E_{rel} = 0.1 kcal mol^{-1}
MIN

B1-B2	1.769	B1-B3	1.784
B1-B4	1.741		
B1-B5	1.769	B1-B9	1.795
B2-B3	1.797		
B2-B5	1.735	B3-B9	1.763
B2-B6	1.751	B3-B8	1.783
B2-B7	1.751	B3-B7	1.818
B4-B5	1.808	B4-B9	1.657
B5-B6	2.007	B8-B9	2.010
B6-B7	1.841	B7-B8	1.894
B4-H^{μ}	1.311	B5-H^{μ}	1.342
B7-H^{μ}	1.277	B8-H^{μ}	1.390
B6-H^{endo}	1.207	B8-H^{endo}	1.211

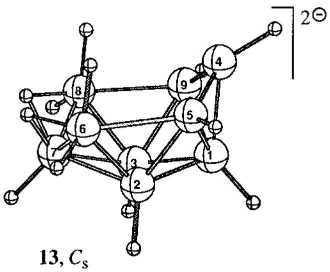

13, C_s
E_{rel} = 34.4 kcal mol^{-1}
MIN

B1-B2	1.743	B2-B7	1.855
B1-B4	1.794	B4-B5	1.653
B1-B5	1.785	B5-B6	2.065
B2-B3	1.809	B6-B7	1.907
B2-B5	1.779	B6-H^{μ}	1.311
B2-B6	1.784	B7-H^{μ}	1.354

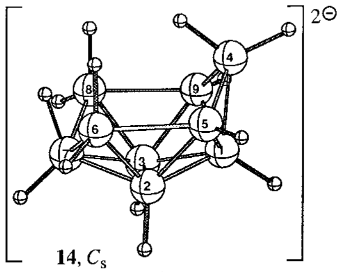

14, C_s
E_{rel} = 7.7 kcal mol^{-1}
SOSP (713i cm^{-1}, A”; 418i cm^{-1}, A”)

B1-B2	1.782	B4-B5	1.787
B1-B4	1.735	B5-B6	1.989
B1-B5	1.732	B6-B7	1.877
B2-B3	1.834	B4-H^{endo}	1.200
B2-B5	1.787	B6-H^{endo}	1.205
B2-B6	1.737	B7-H^{endo}	1.226
B2-B7	1.786		

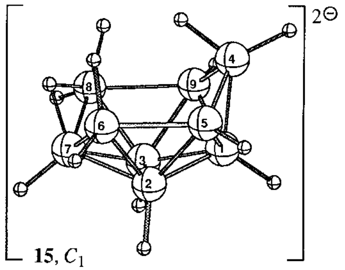

15, C_1
E_{rel} = 4.6 kcal mol^{-1}
TS (267i cm^{-1})

B1-B2	1.764	B4-B5	1.757
B1-B3	1.793	B4-B9	1.808
B1-B4	1.735	B5-B6	1.927
B1-B5	1.768	B6-B7	1.849
B1-B9	1.717	B7-B8	1.881
B2-B3	1.819	B8-B9	2.005
B2-B5	1.736	B7-H^{μ}	1.305
B2-B6	1.741	B8-H^{μ}	1.359
B2-B7	1.766	B4-H^{endo}	1.207
B3-B7	1.814	B8-H^{endo}	1.213
B3-B8	1.754	B9-$H^{endo,B8}$	2.077
B3-B9	1.744	B6-H^{endo}	1.203

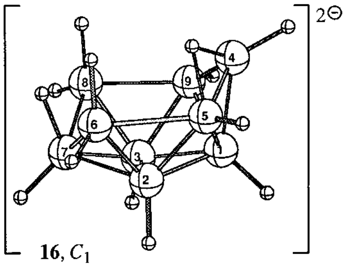

16, C_1
E_{rel} = 2.2 kcal mol^{-1}
TS (383i cm^{-1})

B1-B2	1.782	B4-B5	1.791
B1-B3	1.779	B4-B9	1.661
B1-B4	1.747	B5-B6	2.081
B1-B5	1.746	B6-B7	1.878
B1-B9	1.801	B7-B8	1.908
B2-B3	1.823	B8-B9	1.980
B2-B5	1.743	B4-H^{μ}	1.317
B2-B6	1.748	B5-H^{μ}	1.338
B2-B7	1.767	B6-H^{endo}	1.209
B3-B7	1.786	B7-H^{endo}	1.217
B3-B8	1.757	B8-H^{endo}	1.208
B3-B9	1.747		

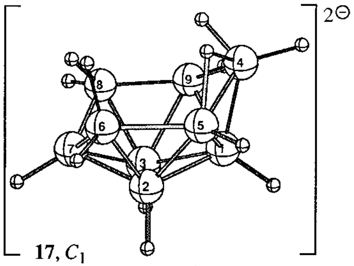

17, C_1
E_{rel} = 3.6 kcal mol^{-1}
TS (273i cm^{-1})

B1-B2	1.789	B4-B9	1.872
B1-B3	1.805	B5-B6	1.832
B1-B4	1.714	B6-B7	1.918
B1-B5	1.809	B7-B8	1.855
B1-B9	1.830	B8-B9	1.722
B2-B3	1.749	B4-H^{μ}	1.300
B2-B5	1.761	B5-H^{μ}	1.381
B2-B6	1.758	B4-H^{endo}	1.260
B2-B7	1.729	B9-$H^{endo,B4}$	1.503
B3-B7	1.732	B7-$H^{endo,B8}$	1.735
B3-B8	1.732	B8-H^{endo}	1.220
B3-B9	1.834	B6-H^{endo}	1.203
B4-B5	1.852		

Figure 6. Geometries optimized at MP2(fc)/6-31G* for various $[B_9H_{13}]^{2-}$ structures **10** to **17**.

Table 7. Computed ^{11}B NMR Chemical Shifts for $[B_9H_{13}]^{2-}$ Structures **10**−**14** in Comparison to Measured Data

	B1		B2, B3	B4		B6, B8	B7		B5, B9
10, C_s	−55.8		−11.7	−24.6		−42.8	−1.1		−5.6
10, C_s, av		−26.4			−36.7			−4.1	
11, C_1	−47.1		4.3, −39.3	3.0		−33.0, −20.4	−37.8		−9.0, 13.9
11, C_1, av		−27.4			−16.8			−11.0	
12, C_1	−54.5		−4.3, −22.1	−4.5		−30.4, −30.7	−43.3		−2.1, 13.2
12, C_1, av		−27.1			−21.9			−10.7	
13, C_s	−40.9		−28.6	5.9		−45.3	−27.0		21.3
13, C_s, av		−32.7			−28.2			5.2	
14, C_s	−32.9		−10.4	−35.0		−19.3	−56.0		39.1
14, C_s, av		−17.9			−25.1			7.4	
av (**10**, **11**, **12**)[a]		−27.0			−24.5			−8.6	
expt[b]		*−29.0*			*−24.9*			*−4.55*	

[a] Equally weighted combined averaged shifts for **10**, **11**, and **12**. [b] K$^+$ salt in ND$_3$ at −40 °C, without assignment, ref 41.

experimental low field signal at −4.55 is reproduced well only by **10**. However, this structure gives a large deviation of 7.7 ppm for the computed B4,6,8 value of −36.7 ppm. The results for **11** and **12** are not satisfactory, either. The best assignments still give maximum deviations of 8 (**11**) and 6 ppm (**12**). While individual shifts for **11** and **12** differ significantly (up to 17.2 ppm for B3), the only significant deviation of the averaged shifts is 5.1 ppm for B4,6,8. Structures **14** and **13** with considerably higher relative energies than **10**, **11** and **12** show even larger chemical shift discrepancies. Averaging over **10**, **11** and **12**, which are very close in energy, gives a set of theoretical shifts (B1,2,3, −27.0; B4,6,8, −24.5; B5,7,9, −8.6) which compare well with the measured values (−29.0, −24.9, −4.55).[41] This suggests that three isomeric structures of $[B_9H_{13}]^{2-}$ may be important in solution: **10**, **11**, and **12**, each of which have two endo terminal and two hydrogen bridges.

This model implies that all three isomers can rearrange into one other very easily. Therefore, we located the transition structures connecting the minima **10**, **11** and **12**. One hydrogen bridge in **11** has to shift in going to **12**. In the corresponding transition structure, this bridging H becomes an endo terminal H at B4 ($B4-H^{\mu}-B9$ shift to $B4-H^{\mu}-B5$) or at B7 ($B7-H^{\mu}-B8$ shift to $B6-H^{\mu}-B7$, which gives the **12** enantiomer). The corresponding transition structures, **15** (267i cm^{-1}) and **16** (383i cm^{-1}) have relative energies of 4.6 and 2.2 kcal mol^{-1}, respectively. The rearrangement from **10** to **11** may occur by $B8-H^{endo}$ bridging to B9 together with a conversion of the B4/B5 bridge hydrogen to $B4-H^{endo}$. (The numbering changes: B8 becomes B4 (and vice versa), B3 becomes B1 etc.) The transition structure search starting with a geometry interpolated between **10** and **11** converged to **15**. On the other hand, the change of $B4-H^{\mu}-B9$ to $B4-H^{endo}$ in **10**, accompanied by the $B8-H^{endo}$ bridging to B7 rather than B9, gives **12** instead of **11**. The corresponding transition structure, **17** (273i cm^{-1}), has a relative energy of 3.6 kcal mol^{-1} (B8 in **10** and **17** becomes B4 in **12**, B5 becomes B7 etc.). These results show that **10**, **11**, and **12** can easily interconvert and that all endo hydrogen atoms can exchange their chemical environments with a maximum barrier of 4.6 kcal mol^{-1}.

Conclusion

The application of the ab initio/IGLO/NMR method to various 9-vertex *arachno* boron hydrides clarifies a number of structural details. The "best" experimental geometry for *n*-B_9H_{15} recommended by Beaudet[29] has satisfactory boron placements but the hydrogen parameters are in error. Not only is the computed energy very high, but the IGLO computed chemical shifts also show large discrepancies with the experimental NMR data in comparison to the results using a fully optimized geometry, **1** (Figure 1).

The *i*-B_9H_{15} isomer favors a C_{3v} structure in solution, **2**, with six strongly asymmetric hydrogen bridges. It is only 2.2 kcal mol^{-1} less stable than *n*-B_9H_{15}. The alternative C_3 proposal[36] with three hydrogen bridges and three endo terminal hydrogen atoms has two imaginary frequencies at HF/3-21G and is not a stationary point at all at higher levels employed.

The C_s symmetric $[B_9H_{14}]^-$ structure, **6**, reported for the solid state,[38b] is found computationally to be a transition structure. The corresponding C_1 minimum, **7**, with the endo hydrogen at B7 bridging to B8, is shown to be the solution structure by comparing the computed with the measured ^{11}B NMR chemical shifts. As the cluster geometries of **6** and **7** do not differ appreciably, the possibility is raised that the additional hydrogen bridge was not recognized in the X-ray structure analysis.

In contrast to expectations, the experimental solid-state geometries of $[B_9H_{14}]^-$ (**6**) and $[B_9H_{13}{\cdot}L]$ (analogous to C_s **9a,b**) are not isostructural.[38] However, the solution structures, computed for $[B_9H_{14}]^-$ (**7**) and $[B_9H_{13}{\cdot}NCMe]$ (C_1, **8b**), are closely related.

Based on X-ray diffraction data in the solid state, the $[B_9H_{13}]^{2-}$ dianion was postulated to have five disordered structures differing in endo H placements.[41] However, two of these have ca. 45 kcal mol^{-1} higher energies and converge to one of the low energy structures when the hydrogen positions are optimized. Hence, we propose that only three disordered structures **10**, **11** and **12** are present in the solid state. Experimental ^{11}B NMR chemical shifts only are reproduced if these three different structures, very close in energy, are taken into consideration. The hydrogen rearrangements which interconvert **10**, **11** and **12** have low barriers of 4.6 kcal mol^{-1} or less.

Acknowledgment. Financial support by the Deutsche Forschungsgemeinschaft (Schwerpunktprogramm Polyeder) and the Fonds der Deutschen Chemischen Industrie is gratefully acknowledged. This paper is dedicated to Prof. W. Kutzelnigg for the development of IGLO, the first practicable *ab initio* method for the computation of magnetic properties.

Supporting Information Available: One table listing absolute energies at the MP2(fc)/6-31G* level for structures discussed in the text. This material is available free of charge via the Internet at http://pubs.acs.org.

IC9714450